Physica B 173 (1991) 17–24
North-Holland

An automated neutron reflectometer (POSY II) at the Intense Pulsed Neutron Source

Alamgir Karim[1], B.H. Arendt[2], Rick Goyette, Y.Y. Huang, R. Kleb and G.P. Felcher
Argonne National Laboratory, Argonne, IL 60439, USA

A brief description is given of the time-of-flight neutron relfectometer POSY II at the Intense Pulsed Neutron Source (IPNS) at Argonne National Laboratory. Both data collection and refinement of the experimental data are nearly automatic. The neutron reflectivity is measured as a function of the neutron momentum perpendicular to the surface over a range from 0 to 0.1 $Å^{-1}$. The instrument is capable of measuring reflectivities as low as 10^{-6}. The neutron reflectivity is used to determine the composition profile of the layers close to the surface of the sample, with a depth resolution of ~10 Å.

1. Introduction

The last decade has witnessed an enormous development of neutron (as well as X-ray) reflectometry [1–4]. The procedure is indeed simple, consisting in measuring the reflectivity of a beam glancing at an angle θ with a surface. The reflectivity is a rapidly decreasing function of $k_z = 2\pi \sin\theta/\lambda$ (where λ is the beam's wavelength) and contains detailed information about the chemical and magnetic profile of the material progressing from the surface into the bulk. This profile is an optical transform of the reflectivity. Both the range (~3000 Å) covered and the resolution (~10 Å) make this technique quite useful and truly complementary to other depth profiling techniques. Additionally, there is the possibility of "coloring" some of the layers either by isotopic (for neutrons) or heavy atom (for X-rays) substitution.

The purpose of the present paper is to provide a detailed description of the reflectometer "POSY II" and its operation. The reflectometer basically consists of an optical table, where a well collimated beam of neutrons strikes a sample at a small angle of incidence ($\theta < 3°$) and a detector where the reflected neutrons are measured. The neutron source is pulsed and the incident beam contains a wide distribution of neutron energies. The time of arrival of a neutron at the detector is proportional to its wavelength. Since the scattering plane of the neutrons is horizontal, and the sample surfaces vertical, POSY II is primarily designed for the study of solid–solid and solid–air interfaces. Samples can come in a variety of different shapes and sizes.

POSY II has been designed as a user friendly instrument: most new users become capable of operating it independently with only a few hours of "hands-on" experience. Only a few minutes are required to set up a data collection run. The user has only to mount the sample on a holder (three-points mounted on a prepositioned goniometer table). A laser beam, permanently installed to closely follow the neutron path, allows a quick optical check of the sample position in the beam and the orientation of its surface. The controlling computer can then execute a sequence of runs, each characterized by certain physical parameters, like the angle of incidence and the beam resolution. A wide variety of displays is available for the collected data, both in raw form and as reflectivity versus k_z.

[1] Present address: Department of Chemical Engineering and Material Science, University of Minnesota, MN 55455, USA.
[2] Present address: Physics Department, California Institute of Technology, Pasadena, CA 91125, USA.

The neutron beam used by POSY II is generated by the Intense Pulsed Neutron Source [5], which consists of a particle accelerator, spallation target, and surrounding moderators and reflectors. H^- ions produced in an ion source are accelerated to 750 keV in a pre-accelerator and then to 50 MeV in a linac. The beam of H^- ions are then magnetically steered to a Rapid Cycling Synchrotron (RCS). At its entrance the H^- pass through a carbon foil that strips the electrons. The resulting proton beam is accelerated in the evacuated ring of the RCS, reaching an energy of 450 MeV after $\sim 10^5$ revolutions. A septum magnet steers 80 ns bursts of protons to strike a neutron spallation target of highly enriched uranium, which "boils off" neutrons in spallation and fast fission processes. The operation has a frequency of 30 Hz.

The fast neutrons produced by the target are slowed down in a liquid hydrogen moderator to an effective mean temperature of 30 K. The cold neutrons are collimated in two evacuated tubes (3 m long) that run from the moderator to two neutron gates. The tubes, in the shape of tapered vertical slits, are carved in solid steel blocks. They feed two independent reflectometers: a polarized neutron reflectometer (POSY I) for magnetic profile work [6] and the one described here. The individual beam gates set at the exit of the collimators consist of pneumatically controlled mini-shutters of tungsten (10 cm length × 10 cm height × 1 cm width). After the gates the neutrons pass through a short (60 cm) collimator, surrounded by borated polyethylene beads. The beam opening for POSY II is 6.6 cm high, 1.1 cm wide, at the face of the biological shielding monolith.

2. Architecture of the reflectometer

An optical bench in front of the biological shield supports the entire reflectometer complex. The layout in fig. 1. shows the main components of POSY II: the neutron filter assembly, the sample table, and neutron detector.

The neutron beam spectrum is reshaped by passing through two reflection filters. The first reflects neutrons of wavelength larger than 2.5 Å; the remaining radiation passes through the filter and is captured in a block composed lf lead and borated polyethylene. This radiation consists of the high energy part of the quasi-thermalized incident neutron spectrum as well as the flash of high energy radiation (gamma rays and fast neutrons) emitted at the time, t_0, when

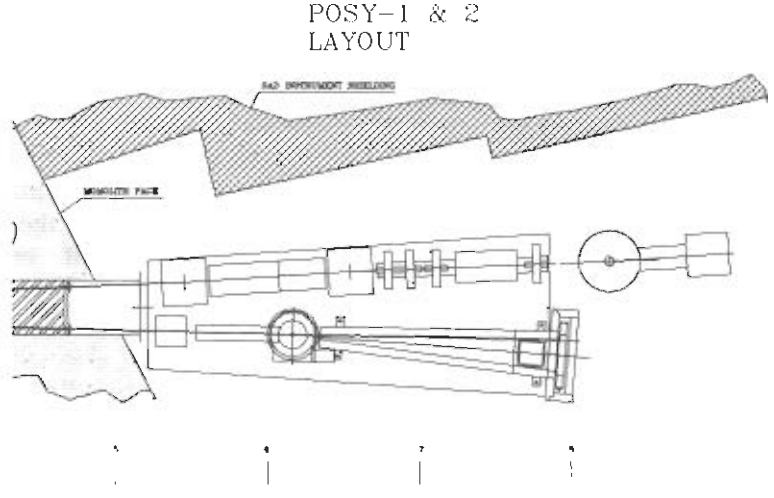

Fig. 1. Layout of the reflectometer complex at IPNS, as viewed from the top. The polarized unit POSY I is on the upper section of the optical bench. Well visible are the round sample goniometer of POSY II and the wedge-shaped housing of the detector. Indicated below the figure is the distance from the moderator (in meters).

the proton beam strikes the target. The filter consists of a stack of silicon wafers (10 cm diameter × 0.5 mm thick) coated with isotopic ^{58}Ni (~1000 Å on both sides). The wafers totally reflect neutrons of wavelength larger than 2.5 Å, when set at an angle of 0.3° to the incident beam. Each wafer reflects a slice of the incident beam 0.5 mm wide. In order to reflect the entire beam, twelve wafers are stacked as in a Soller collimator, and sandwiched between two 2.5 cm thick optical flats pressed between spring mounted aluminum plates. Micrometers provide accurate translation and rotation of the assembly.

The role of the second filter (fig. 2) is to reflect out of the incident beam long wavelength neutrons that would have arrived at the detector during subsequent time frames. With a repetition frequency of 30 neutron pulses per second, and a source–detector distance of 8.9 meters, the frame overlap neutrons have a wavelength λ greater than 16 Å. Note that even if these slow neutrons are relatively few (because they are in the tail of a Maxwellian distribution (fig. 3)), their reflectivity is often higher by several orders of magnitude than that of the short wavelength neutrons detected simultaneously. As a result, the reflectivity would be artificially increased at high momentum values. The filter, a single wafer of silicon coated with ^{58}Ni, is positioned on the beam line at an angle of 1.8°.

The reflection filters are coated with ^{58}Ni because this isotope makes the most reflecting single coating mirror, with a critical angle $\theta_c = 0.12°$ for 1 Å neutrons (and linearly increasing with the wavelength). Presently under test are supermirrors [7] (to increase the beam luminosity incident on the sample) made of multiple graded coatings of nickel and titanium, which should extend the region of total (or almost total) reflectivity by at least a factor of two.

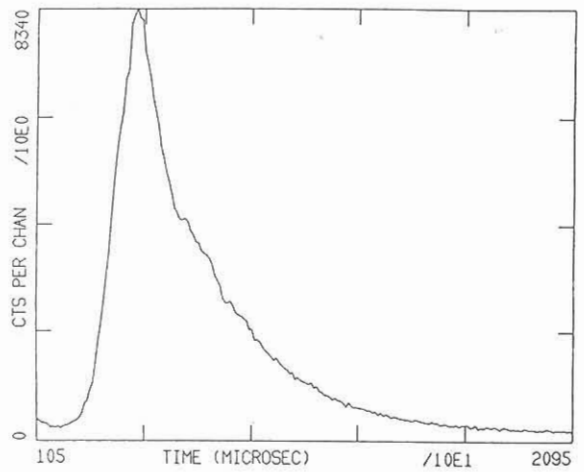

Fig. 3. The time-dependent spectrum of the neutron beam, as seen by the neutron detector. To convert to wavelengths, $\lambda(\text{Å}) = 5 \times 10^{-4} t\,(\mu\text{s})$.

The angular resolution of the beam is controlled by two slits 72 cm apart. The slits (3 mm wide, 63 mm high) are cut through the center of vertical cylinders of boron nitride, of 12 mm diameter. The width of the transmitted beam is

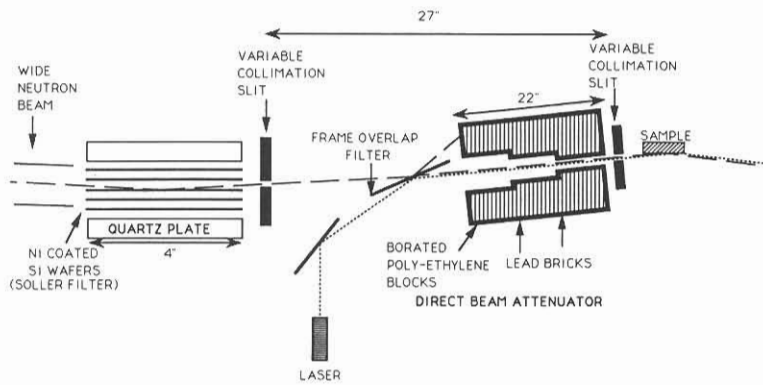

Fig. 2. Details of the filter/collimation system of POSY II.

varied by rotating the cylinders on their axis with the aid of stepping motors under computer control. The motors have 400 steps per turn, and their rotation is divided by two stage reducing gears ($\frac{1}{20}$, $\frac{1}{6}$) to give a minimum rotation of the slits of 4.3″, which corresponds to a variation of the beam width of $\frac{1}{4}$ μm.

Normally the two slits are opened in tandem, providing a divergence $\Delta\theta$ of the incident beam adjusted to the angle of incidence of the beam on the sample. In normal operation the angular resolution ($\Delta\theta/\theta$) is kept fixed in runs at different $\theta(\Delta\theta/\theta \sim 0.05)$. Since this is the leading term of the total instrumental resolution, data sets collected at various angles of incidence can be directly compared or merged to obtain the reflectivity over a larger momentum range. The results can even be compared with the reflectivities calculated for model profiles, and smeared by a prefixed divergence. An added advantage of the variable collimation is that the data collection rate is increased in the large angle, low reflectivity region, because the beam width is automatically adjusted to illuminate the same area of the sample surface.

The sample is rotated by a single axis Huber goniometer with a 0.005° precision. On top of the goniometer is a table equipped with a micrometer for high precision translation perpendicular to the incident beam axis. Locating pins on the micrometer table permit the rapid change of different sample cells. The original cell was a rectangular aluminum box with entrance/exit Mylar windows [8]. The cell accepts sample mounts designed to hold circular samples of diameter 5 cm or rectangular samples of dimensions 4 × 8 cm. The mounts can be reproducibly set in place with a three point contact with the sample cell. The samples are gently pressed against front reference plates (at the top and the bottom) by a spring loaded back plate. In the case of the circular mount, the back aluminum plate is threaded to allow for substrate thicknesses ranging from 3 to 14 mm. The sample cell also accepts an insert, in which round samples of 2.5 cm diameter can be cooled down to −60°C. A computer controlled sample changer is presently being tested (fig. 4).

The detector assembly consists of a ^{3}He gas filled linear detector with a 70% efficiency for 3 Å neutrons [9]. Its sensitive electrode is a 200 mm long quartz rod coated with carbon. The carbon coating acts as a resistive element assuring a linear resolution of better than 1.5 mm. The detector is placed at a distance of 175 cm from the sample, subtending an angle $2\theta = 6°$. For primary shielding, the detector is surrounded by a 12 mm thick boron carbide sheath. Both

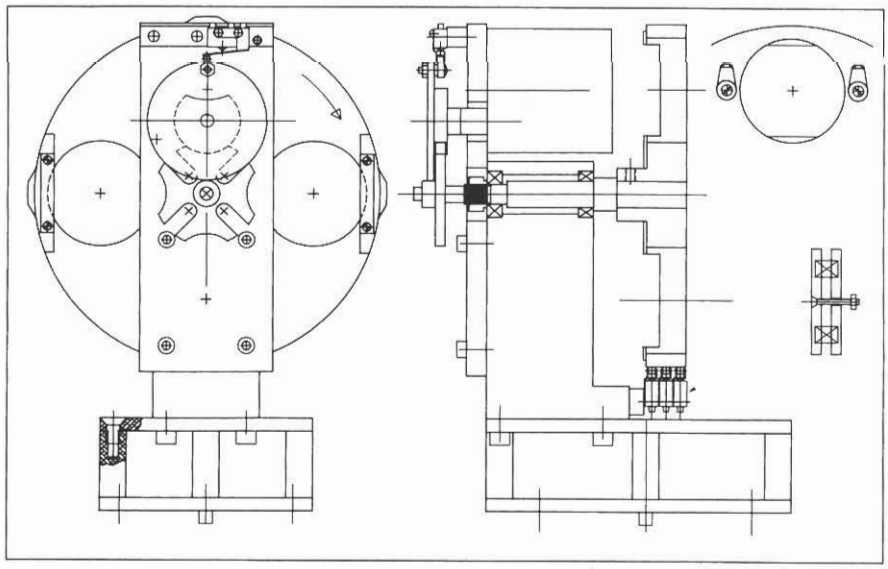

Fig. 4. The sample changer. Four samples are rotated into position by a Geneva drive.

detector and final flight path are enclosed in a wedge shaped masonite box with 5 cm thick walls with all internal surfaces sheathed with cadmium. Reflected neutrons enter the sealed box through a Mylar window. ^{4}He is circulated through the box to minimize stray neutron scattering. The transmitted beam is blocked by a movable boron nitride mask, 4 cm wide, placed in front of the detector both to prevent dead time corrections and to prolong the life of the counter (the carbon coating which constitute the counter anode eventually evaporates from the quartz wire). The mask limits the reflection measurements to angles of incidence $\theta > 0.2°$. When measuring the incident spectrum, the mask is raised, but the intensity of the direct beam is attenuated by a series of horizontal slits.

3. From neutron detection to reflectivity

The linear-sensitive detector is connected to a Vax Station II/GPX computer. The 256 position (x) channels of the detector have uniform width, as revealed by the flood pattern of an isotropic neutron source. Each position channel is divided into 256 time of flight channels. The neutron wavelength depends on time as $\lambda(\text{Å}) = 4.0 \times 10^{-3} \times t(\mu\text{s})/d(\text{m})$; d is the moderator–detector distance, and t is the time as measured from t_0. The value chosen for d (7.9 m), represents a compromise. Setting the detector closer to the moderator would increase the range of usable wavelengths. However, the tight angular resolution required in neutron reflectometry can be best achieved by increasing the moderator–sample and sample–detector distances. Data are collected for times from 4 to 33 ms, which correspond to neutron wavelengths between 2 and 16 Å. The width of the time channels is set to increase linearly with time maintaining constant time resolution. With $\Delta t/t = 0.01$, the time resolution is considerably smaller than the angular resolution.

The intensities collected versus x and t can be viewed in a 3-dimensional plot, or in a to-

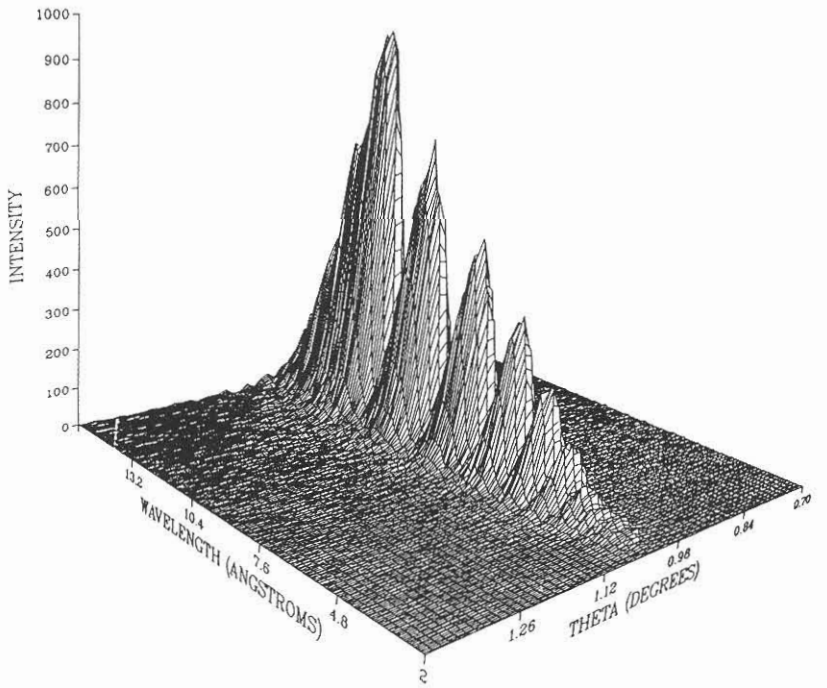

Fig. 5. Three-dimensional plot of the intensity reflected by a sample consisting of a 1000 Å thick deuterated polystyrene on a silicon wafer. At long wavelengths, the reflectivity is unitary. The periodic oscillations at shorter wavelengths are due to the interference of the beams reflected by the top and bottom of the film.

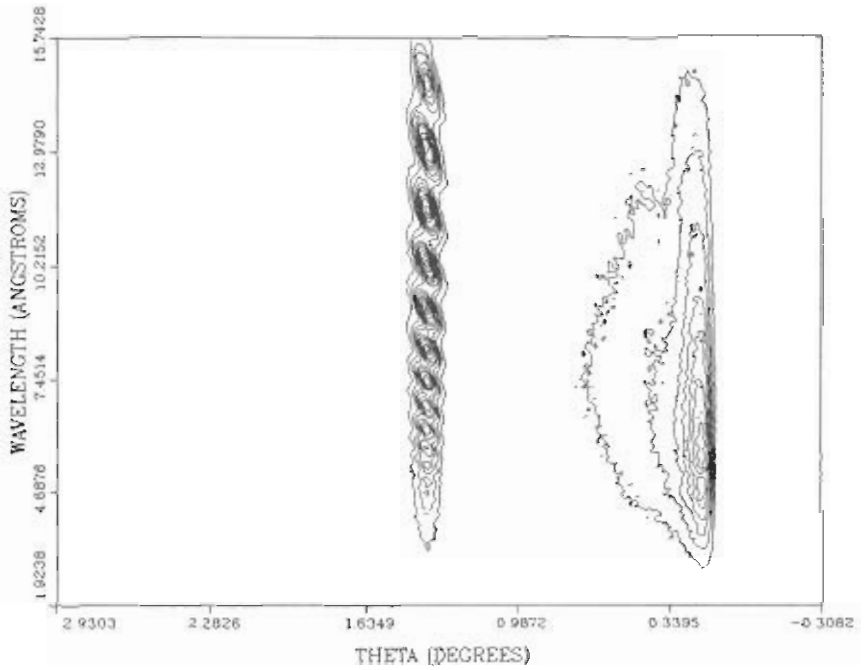

Fig. 6. Contour plot for a sample similar to that presented in fig. 5. The wide band of intensity at the right represents neutrons refracted by the substrate.

pographical manner as a contour plot. As an example, figs. 5 and 6 present the data obtained from a later of deuterated polystyrene, 1000 Å thick, on silicon. These relatively complex pictures contain all the recorded intensity from neutrons specularly reflected, refracted and scattered. Usually only part of the data is viewed. For instance, by selecting a t-channel, an intensity as a function of position histogram can be generated (fig. 7) from which the position x_0 of the reflected peak can be derived very accurately. By looking at a fixed detector element, the peak intensity of the reflected beam can be observed as a function of time (fig. 8).

The calculation of the reflectivity involves several steps. The first is the identification of the reflected peak's detector position, and the evaluation of its intensity versus time (after subtracting the background and the scattered, rather than reflected, intensity). After performing a further correction for delayed neutrons (a correc-

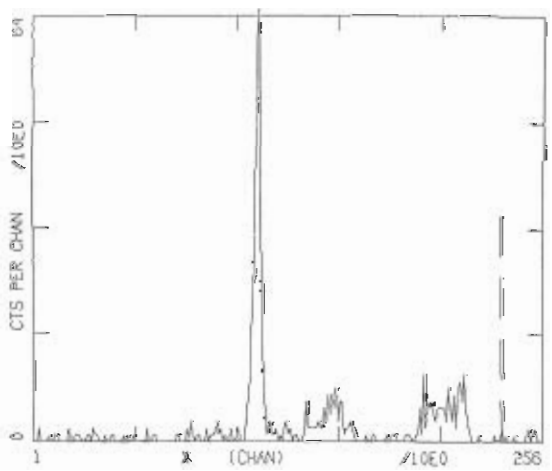

Fig. 7. Intensity of 6 A wavelength neutrons as a function of position on the linear detector. The 256 channels corresponds to the entire detector length of 20 cm. The sample is a film of deuterated polymer. The diffuse scattering at the right side of the reflection line is caused by roughness of the sample surface. The dashed line indicates the position of the incident beam (which has been blanked out).

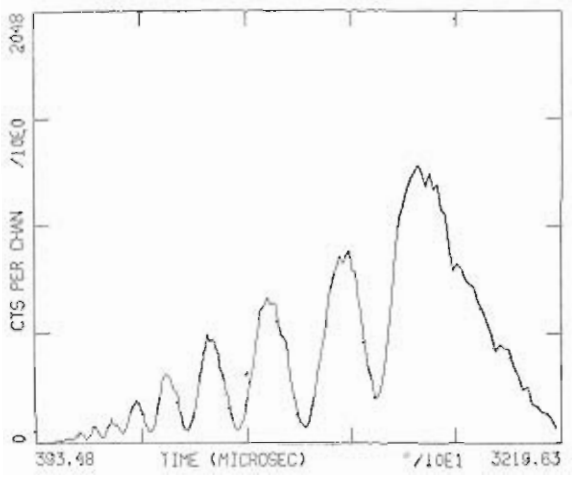

Fig. 8. Intensity of the neutrons reflected in channel 112 (fig. 7) as a function of the time of arrival at the detector.

tion intrinsic to the spallation target used), the intensities must be normalized by the incident flux and read as a function of k_z. These steps, although quite simple, are not entirely trivial.

Normally the reflection peak has a width spanning several x-channels, with individually recorded intensities. For good samples, the background to be subtracted is low. However, roughness at the interfaces or imperfections in the layering may give rise to appreciable scattered intensity in x-channels surrounding the reflected peak. Separation of the reflected from the scattered intensity might be difficult: the x-position of the reflected beam is t-independent, while the centroid of the scattered beam shifts with t until (at least in certain cases) it merges with the reflected beam.

Not all the neutrons detected at time t have a definite wavelength λ. In a target of enriched ^{235}U, "delayed" neutrons are produced as a result of gamma decay of the fission products. With time constants on the order of a few seconds (practically infinite compared with the pulse frequency), these neutrons give a constant background with the same wavelength spectrum as the pulsed beam. The total amount of delayed neutrons has been measured as 2.83% of the entire spectrum. This time independent contamination can be calculated numerically and subtracted. Its contribution to the measured signal becomes quite noticeable for the long wavelength tail of the Maxwellian distribution.

The normalization of the reflected intensity to the incident flux can be obtained in several ways. On POSY II the standard procedure is to normalize the reflected intensity by that obtained for the incident beam, as measured by the same detector with no sample present and tight beam collimation. Care is taken that the moderator temperature does not change between runs. The ratio of reflected to incident beam is then normalized, assuming that for long wavelengths there is a region of total reflection, $R = 1$.

At this stage reflectivity curves have been obtained for each of the x-channels included in the reflection peak. The width of the reflection peak is a combination of the linear resolution of the counter, the width of the neutron beam, and its angular divergence. The last quantity is determined by the distance between the innermost slit collimator and the sample (120 cm) and the slit width, which is variable. Each x-channel corresponds to a slightly different angle, which implies that for a given neutron wavelength the corresponding reflectivity is for a slightly different value of k_z. This is why the reflectivity maxima in the contour plot (fig. 6) have a striped pattern. A composite $R(k_z)$ with improved resolution is generated by the analysis codes. As a last step, the reflectivities for different k_z ranges, obtained from different orientations θ of the sample, are merged. The absolute scale of the reflectivity is preserved only for the lowest θ run,

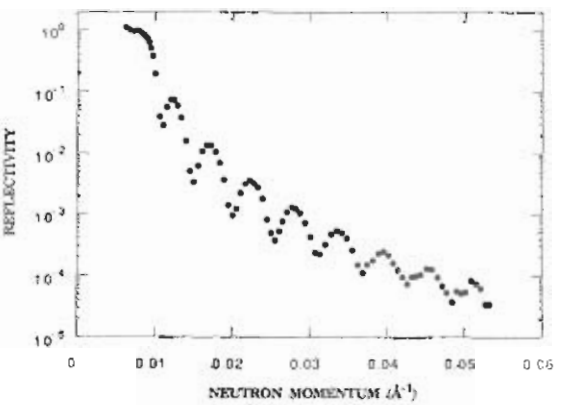

Fig. 9. Normalized reflectivity of the deuterated polymer film already viewed in figs. 6–8.

which is assumed to contain a region where $R = 1$. The runs at higher angles are scaled to match the reflectivities in the regions overlapping those of the lower angle runs. An example of the normalized reflectivity versus momentum for a polymer monolayer on a silicon substrate is shown in fig. 9.

4. From reflectivity to depth profile

The experimental reflectivity is compared with that calculated for model profiles. In principle, the calculation involves the numerical solution of the neutron wave function in a potential proportional to the scattering length density of the depth profile. Having approximated the potential with a histogram of equal height, variable length elements, the solution is obtained by calculating the reflection matrix [10] for each subsequent element boundary. In practice an equivalent algorithm, where the reflectance at each boundary is calculated in a recursive relation [11], requires considerably less computer time. An added advantage of the recursive formula is that it explicitly contains the reflectances of the individual interfaces, which can be independently altered as necessary, for instance to take into account their smoothing due to interdiffusion. [12]

The process of fitting the experimental reflectivity to that calculated for model profiles is quite tedious and lengthy, and at present no common techniques such as least square fitting, have demonstrated much success. In part this difficulty is due to the fact that the optical transformation from profile to reflectance becomes highly nonlinear in the region where the reflection is total. The main guidelines for proposing and refining a model profile have come with the expansion of the expression for the reflectivity for different regions of k_z [2, 13]. This procedure has indicated which of the model parameters are most important in each region [14] and even the hierarchy of their importance [15]. It is our hope that this workshop has proposed, or at least stimulated the discovery of a faster, more systematic method to interpret the data measured with this optical probe.

Acknowledgements

This work was supported by the US Department of Energy, BES-Material Sciences, under contract W-31-109-Eng-38.

References

[1] J.B. Hayter, R.R. Highfield, B.J. Pullman, R.K. Thomas, A.I. McMullen and J. Penfold, J. Chem. Soc. Faraday Trans. 77 (1981) 1437.

[2] G.P. Felcher, Phys. Rev. B 24 (1981) 1595.

[3] B. Farnoux, in: Neutron Scattering in the Nineties, Conference proceedings, IAEA, Vienna (1985) p. 205.

[4] M. Stamm and C.F. Majkrzak, ACS Pol. Preprints 28 (1987) 18.

[5] G.H. Lander and J.M. Carpenter, in: Neutron scattering in the Nineties, Conference proceedings, IAEA, Vienna (1985) p. 17.

[6] G.P. Felcher, R.O. Hilleke, R.K. Crawford, J. Haumann, R. Kleb and G. Ostrowski, Rev. Sci. Instr. 58 (1987) 609.

[7] J.B. Hayter and H.A. Mook, Proc. Conf. on Thin Film Optical Devices, San Diego, 16 August 1988, SPIE, Vol. 983 (1988).

[8] The cell was designed and built at IBM Almaden by T.P. Russell and A. Karim.

[9] Manufactured by: Ordela Inc., 139 Valley Court, Oak Ridge, TN37830.

[10] M. Born and E. Wolf, Principles of Optics (Pergamon, Oxford, 1975).

[11] G. Parratt, Phys. Rev. Lett. 94 (1954) 359.

[12] A. Karim, A. Mansour, G.P. Felcher and T.P. Russell, Phys. Rev. B 42 (1990) 6846.

[13] S. Dietrich and R. Schack, Phys. Rev. Lett. 58 (1987) 140.

[14] R.J. Composto, R.S. Stein, E.J. Kramer, R.A.L. Jones, A. Mansour, A. Karim and G.P. Felcher, Physica B 156 & 157 (1989) 434.

[15] S.S.P. Parkin, V.R. Deline, R.O. Hilleke and G.P. Felcher, Phys. Rev. B 42 (1990) 10583.